AN EFFECTIVE DEEP LEARNING BASED APPROACH TO MEASURE INTERDEPENDENCE OF HEART RATE VARIABILITY ANALYSIS AND R-PEAKS

M.B. Shananawaz[1] and H. Dawood[1*]

[1]Department of Software Engineering, University of Engineering and Technology, Taxila
[*]Corresponding author's E-mail: hassan.dawood@uettaxila.edu.pk

ABSTRACT: Heart rate variability (HRV) is the physiological phenomenon to measure variations between consecutive heartbeats. HRV analysis has been used to analyse and detect different cardiac diseases that rely on R-peaks' reliability and accurate detection. Myocardial infarction (MI) is a main cardiac disease that causes irregularity in heartbeats and some non-specific abnormalities occur in the recorded ECG, including ST changes and T-wave alternans. These abnormalities may be ignored by considering minor changes that can lead to delayed diagnosis. Therefore, the analysis of these abnormalities is a challenging task. This study investigated these non-specific abnormalities to recognize MI patterns based on HRV analysis highlighting the importance of R-peaks detection accuracy. Short-term HRV analysis of two publicly available datasets, MIT-BIH ST Changes and European ST-T changes was performed based on R-peaks detected from ECG signals. R-peaks detection achieved an averaged 99.77% sensitivity, 99.49% positive predictability and 99.32% accuracy for MIT-BIH ST changes dataset whereas for European ST-T changes dataset, 99.85% sensitivity, 99.41% positive predictability, and 99.28% accuracy was achieved. Subsequently, HRV parameters were computed from both datasets and data fusion was performed followed by a deep learning model to find out the most accurate pattern recognition results. For pattern recognition, a finely tuned artificial neural network was applied to HRV parameters, in two scenarios. For both scenarios, an accuracy greater than 99% was achieved. Furthermore, linear regression was also performed on computed HRV measures in both scenarios that observed a similarity of 97% between both datasets. The importance of reliable and accurate R-peaks detection for HRV analysis to analyse and detect different cardiovascular diseases was elaborated in the end.

Key words: Deep learning, Electrocardiogram, Heart rate variability analysis, ST-T changes, R-peaks detection.

(Received 01.10.2021 Accepted 01.06.2021)

INTRODUCTION

Heart rate (HR) measures the average heartbeats per minute based on the R-peaks of the primary Electrocardiogram (ECG) signal. The variation in normal rhythm of heartbeats causes irregularities that indicate current cardiac disease or warns about an imminent disease. This irregular behaviour may result in bradycardia or tachycardia and HR increases or decreases from the normal scale (Kora and Kalva, 2015). Heart rate variability (HRV) is the physiological phenomenon to measure this variation of time interval between consecutive heartbeats that depends upon the regulation of the HR (Jovic *et al*., 2019). It reflects modulation of the normal rhythm of the heart and provides a means to assess the interaction between sympathetic and parasympathetic activities of the autonomic nervous system (ANS). Escalated sympathetic activity and impaired parasympathetic activity causes cardio-acceleration that increases HR and decreases HRV. Conversely, increased parasympathetic activity and lower sympathetic activity results in cardio-deceleration and results in decreased HR and increased HRV (Acharya *et al*., 2006). The balance between both activities controls the HR. The degree of variation in HR depicts the heart's ability to respond and preliminary depends upon the R-peaks from the QRS complex.

Cardiovascular diseases (CVDs) is a category of disorders that affects the heart and blood vessels (Organization, 2017). The main group of CVDs related to heart is coronary heart disease (CHD) which occurs due to blockage of the major blood vessels which are responsible for the supply of blood, oxygen, and nutrients to the heart. According to the World Health Organization (WHO), CVDs are the leading cause of deaths and approximately 17.9 million people die per annum because of CVDs which contributes almost 31% to all deaths worldwide. 85% of these CVD deaths are due to heart attacks and strokes. In 2015, 17 million premature deaths were recorded because of non-communicable diseases and 37% of these deaths were caused by CVDs (Organization, 2017). According to a report from the American Heart Association (AHA), approximately 92.1 million adults in United States of America have at least 1 type of CVD of which 43.8% are having CHD, and every 40 seconds, someone dies due to heart attack.

Consequently, 135 million which is almost 45% of the US adult population is forecasted to suffer from any of CVDs by 2035 (Benjamin *et al*., 2019). Myocardial Infarction (MI), conventionally known as heart attack is a CVD due to lacked supply of blood or oxygen to heart muscles. This prolonged lack of supply damages muscles and continues damage proceeds to irreversible death of muscles leading to MI (Baloglu *et al*., 2019, Anderson and Morrow, 2017, Thygesen *et al*., 2018). Therefore, timely detection of CVDs is significant to save human lives.

ECG is a distinctive and suitable non-invasive tool to assess the electrical activity of the heart and to diagnose cardiac diseases (Lee *et al*., 2018, Acharya *et al*., 2017b, Iqbal *et al*., 2018, Butun *et al*., 2020). ECG signal consists of some characteristic waveforms partitioned into P-wave, QRS waveform, and T-wave and some segments PR segment, QT interval, and ST-segment (Yakut and Bolat, 2018, Lodhi *et al*., 2018, Iqbal *et al*., 2018). All components represent different functions and provide significant information to diagnose heart disease. Based on ECG analysis, there are two indicators of MI (Baloglu *et al*., 2019, Basit *et al*., 2019, Clinic): ST-elevation Myocardial Infarction (STEMI) and Non-ST Elevation Myocardial Infarction (NSTEMI). Complete blockage in blood supply elevates the ST segment from its normal position for a healthy subject and causes a STEMI pattern. NSTEMI patterns occur due to partial or temporary blockage and is considered less dangerous (Ahmed, 2015). NSTEMI pattern shows ST depression and T wave alteration in ECG. Collectively these ST changes and T wave changes are named non-specific ST-T abnormalities (NSSTTA) and are ignored by considering just subtle changes (Al-Zaiti *et al*., 2017, Rivero *et al*., 2019, Aro *et al*., 2012, Prutkin, May 2020). Here, HRV plays a pivotal role in the primary screening of impaired cardiac health (Acharya *et al*., 2006) by analysing these non-specific ST-T changes. In HRV analysis, QRS complex detection, specifically R-peaks detection and its interpretation is the crucial step as the analysis is based on intervals between successive R-peaks, known as R-R intervals.

In this study, the relationship between HRV analysis and R-peaks is assessed to analyse the effect of correct and reliable detection of R-peaks. The basic aim is to detect R-peaks from ECG signals with nonspecific abnormalities, to be further used in HRV analyses. Therefore, ECG recordings of the MIT-BIH ST-changes (Albrecht, 1983) and European ST-T Database (Taddei *et al*., 1992) are analysed to detect R-peaks using Hilbert transform (Prasad and Varadarajan, 2013) with the help of RRAPET software (McConnell *et al*., 2020). Furthermore, time-domain parameters for short-term HRV analysis are calculated for both datasets, and the fusion of these features is performed in MATLAB for pattern recognition using a basic deep learning model. The key contributions of this study are as under:

- Time-domain HRV analysis parameters are computed based on detected R-peaks from two datasets.
- The features extracted from both datasets are fused in two scenarios for pattern recognition and results evaluation.
- A customized artificial neural network (ANN) with ten hidden layers and Levenberg-Marquardt algorithm is used to recognize patterns in both scenarios.
- State-of-the-art evaluation matrices are computed to evaluate R-peaks detection results.
- A comparative study is performed to conclude that reliable detection of R-peaks results in better HRV analysis and pattern recognition.
- Linear regression is also performed to analyse the relationship between both datasets.
- Finally, the importance of reliable detection of R-peaks to detect CVDs is highlighted from literature.

The rest of the article is arranged as follows: Various state-of-the-art R-peaks detection approaches are elaborated in the second section. A brief description of the proposed methodology including datasets details, R-peaks detection, and adopted technique to detect R-peaks, HRV analysis parameters, and customized ANN is presented in section three. Section four presents the experimental setup, results and discussions to highlight the importance of R-peaks for the analysis of CVDs whereas the fifth section concludes the study.

RELATED WORK: Over the years, numerous researchers have developed several HRV analysis systems based on R-peaks detection (Chen *et al*., 2017, John *et al*., 2015). So, various R-peaks detection methods have been proposed using different combinations of filtering and morphological operations, transform methods, derivative methods, template matching, and decision making. The very first and well-known method for peak detection is the Pan-Tompkins method (Pan and Tompkins, 1985) developed in 1985, which is the benchmark for R-peaks detection. This method depends upon the amplitude, width, and slope of the ECG signal. In pre-processing phase noise is removed, the waveform is smoothed and QRS width and the slope is amplified followed by two thresholds application to detect true positive R-peaks. A variant of the Pan-Tompkins method (Hamilton and Tompkins, 1986) followed the same pre-processing technique however used adaptive thresholding to optimize the decision rules. For this, three estimators; mean, median, and peak value were used. After this, different techniques are developed until now for R-peaks detection and some main techniques are described here, in chronological order.

(D'Aloia *et al*., 2019) proposed a six staged effective approach to detect and localize R-peaks in ECG. After the pre-processing stage, the Hilbert transform technique followed by thresholding was applied to detect zones having R-peaks in signal and these identified zones were analysed to detect peaks using wavelet transform. (Pang and Igasaki, 2018) proposed an algorithm following the idea that ECG signal is a pictorial depiction of the heart's electrical activity and applied simplification methods from computer graphics to reduce data. Bitmap images were converted into vector images using the vectorization process. After that, signals were marked with eleven different types of slopes and arranged in a sequence. Later, these sequential slopes were represented by a series of alphabetic symbols recognizable by a finite automata recognizer. In the end, the probabilistic analysis was performed to exclude false-positive R-peaks detection. (Yakut and Bolat, 2018) proposed a two-staged R-peaks detection technique as pre-processing followed by decision making. In the pre-processing stage, unwanted frequency components were suppressed by a band-pass filter. Subsequently, squaring operation enhanced these filtered signals and a moving-average filter was used to integrate and smoothen the enhanced signal. Finally, dynamic thresholding was incorporated to detect R-peaks. For R-peaks detection, the time-interval R-R, between each pair of two successive R-peaks was compared to identify the true R-peaks. (He *et al*., 2017) proposed a four staged real-time QRS detection algorithm. In pre-processing, a band-pass filter was used to suppress interference and noise from the signal. QRS complex was enhanced by applying a five-point first-order differential equation followed by absolute and backward accumulation operations. Finally, k-nearest neighbour and particle swarm optimization (PSO) methods were implemented to locate peaks in ECGs having different morphologies. (Qin *et al*., 2017) proposed a time-efficient and adaptive algorithm to detect R-peaks. ECG signals were enhanced by applying wavelet transform multiresolution analysis and negative peaks were converted into positive ones by using signals mirroring to avoid missing detections. After that, the first-order forward differential approach was used to calculate local maxima and was trimmed by applying amplitude and time interval thresholding to locate actual R-peaks.

(Sabherwal *et al*., 2017) used wavelet transform and derivatives followed by Hilbert transform for R-peaks detection. Wavelet transform followed by first and second derivative was applied to enhance QRS complex and to remove artifacts, P and T wave. Afterward, a high-frequency signal was added for QRS complex enhancement and Hilbert transform was applied to detect R-peaks using adaptive thresholding. The noise existed in the primary signal makes accurate extraction of features difficult, so, (Kaur and Rajni, 2017) adopted a hybrid linearization technique and applied an extended Kalman filter in conjunction with the discrete wavelet transform for de-noising. After de-noising, the principal component analysis was applied to locate true R peaks from the noise-free signal. (Sharma and Sunkaria, 2016) proposed a technique with minimal pre-processing and used simple decision rules. A median filter was applied to remove artifacts and Savitzky–Golay filter to smoothen the signal which minimizes the least-squares error. The ECG signals were cubed which enhanced QRS wave amplitude more than P, T waves, and other noises and artifacts. After that, the root mean square was calculated from the cubed signal for decision making. Finely, Kurtosis was used to detect R-peaks from signals with prominent T waves. (Rakshit *et al*., 2016) presented a multi-staged methodology to overcome the nonstationarity of QRS complex and noise. Firstly, the band-pass filter was used to suppress noise existed in the ECG signal and the QRS complex was enhanced using first-order differential followed by amplitude normalization. In the second stage, Shannon energy envelope was extracted and smoothed by passing the signal through a zero-shift moving average filter. In the final stage, true R-peaks were detected without using any thresholding. (Chanwimalueang *et al*., 2015) used matched filtering along with the Hilbert transform to ascertain the resemblance between a template and probable QRSs complex patterns and to locate R-peaks. A dynamic time window was used to eliminate ambiguous R-peaks, based on the standard deviation of detected R-R intervals. Thereafter, the correlation was calculated between the selected QRS template and potential QRSs to select R-peaks.

The basic purpose of all these aforementioned approaches was to improve the accuracy of R-peaks detection algorithms. These algorithms are yet unable to achieve satisfactory performance because of various morphologies that occur in ECGs and the non-stationary nature of the signal. Healthcare systems deal with such risk factors that minor details like non-specific abnormalities of heart activities become significant to analyse. These non-specific changes may also distract the reliable detection of R-peaks. Therefore, detection of R-peaks from ECG signals having non-specific abnormalities becomes a challenging task as the reliability of HRV analysis is based on these detected R-peaks.

MATERIALS AND PROPOSED METHODOLOGY

ECG Datasets: In this study two data sets, MIT-BIH ST-changes (Albrecht, 1983) and European ST-T Database (Taddei *et al*., 1992) were used, publicly available on PhysioNet (PhysioNet). MIT-BIH ST-changes database

contains 28 ECG records with varying lengths recorded from two different channels. Most of the records were recorded during exercise and exhibit temporary ST depression whereas the last few records were segments taken from long-term ECG recordings and exhibit ST elevation. All of the records have data files, annotation files, and header files containing information about ECG records. The annotation files have all labelled beats by experts and are used to detect R-peaks in each record. Each record was sampled at 360 samples per second.

European ST-T Database contained 90 annotated ECG records from two channels (LIII and V4) for 79 subjects with a length of two hours, where few records were repeated from the same subjects. Subjects included 70 men with an age interval of 30 to 84 and 8 women with an age interval of 55 to 71 whereas information for one subject was missing. Each patient was diagnosed with or suspected for MI; additionally, the selection criteria was based on ECG abnormalities like ST segment displacement and/or T-wave altered due to ventricular dyskinesia, hypertension, and/or effects of medication. All the records have data files, header files with information about subjects, their disease, and medication along with recording channels. Annotations files were also associated with each record containing annotations for each beat as well as annotations for ST-segment changes and T-wave morphological variations. All the abnormalities were properly labelled by two cardiologists independently and all the conflicts were resolved. The database consists of 367 episodes of ST-segment change exhibiting ST elevation or ST depression whereas 401 episodes of T-wave changes with a duration of 30 seconds to several minutes. Each record was sampled at 250 samples per second with a 12-bit resolution over a nominal 20 millivolt input range.

Adopted Technique for R-peaks detection: The Hilbert transform, $H_s(t)$, of a signal s(t), is interpreted as:

$$H_s(t) = s(t) * \frac{1}{\pi t} = \frac{1}{\pi} \int_{-\infty}^{+\infty} \frac{s(t)}{t-\tau} d\tau \qquad (1)$$

Therefore, $H_s(t)$ is a time dependent linear function of s(t) which is acquired by the convolution of s(t) with the signal $(\pi t)^{-1}$. Eq. 1 shows that $H_s(t)$ is the response of linear time-invariant filter i.e. called Hilbert Transformer, with impulse response of $(\pi t)^{-1}$, to s(t). Hilbert transform is usually denoted as ˆg(t). It's easier to understand Hilbert transform in the frequency domain rather than time domain, so, assuming the frequency domain and applying the Fourier transform results as following:

$$F\{H_s(t)\} = -j\, sgnF\{s(t)\} \qquad (2)$$

Where j is an imaginary unit and signal has Fourier transform:

$$sgnF\{S(t)\} = \begin{Bmatrix} -j, & if\ f > 0 \\ 0, & if\ f = 0 \\ j, & if\ f < 0 \end{Bmatrix}$$

Therefore, the Hilbert transform changes the phase of all positive frequency components by $-\frac{\pi}{2}$ and for all negative components phase changes by $+\frac{\pi}{2}$ whereas the magnitude of F{s(t)} remains constant. Thus the Hilbert transform exchanges the real and imaginary parts of F{s(t)}. The function s(t) and its transform $H_s(t)$, both are associated with each other and create an analytic signal expressed as:

$$Z(t) = s(t) + j\mathrm{Hs(t)} \qquad (3)$$

The magnitude of z(t) is:

$$m(t) = \sqrt{s^2(t) + H_s^2(t)} \qquad (4)$$

It's obvious from Eq.4 that s(t) and m(t), both have common tangents and the same value at the point where $H_s(t)$ is zero. In fact, m(t) has the same magnitude and slope of signal s(t) at/near to its local maxima. Consequently, the maximum contribution to the magnitude at points, when s(t)=0, is given by the Hilbert transform.

Methodology: The proposed methodology was built on R-peaks detection, HRV features extraction, data fusion, and artificial neural networks (ANNs) for pattern recognition. The simple and systematic operational flow of methodology is shown in Figure 1. The first step was R-peaks detection which took ECG signal as input to detect peaks after performing some pre-processing. Twenty records from each dataset were used to detect R-peaks and calculate evaluation matrices. Subsequently, short-term HRV analysis parameters were measured for both datasets and data fusion was performed in two scenarios. In the first scenario, HRV features from MIT-BIH ST-changes dataset were used as input cases whereas HRV features from European ST-T Database were used as target cases. In the second scenario, the same procedure was applied whereas the input case and target case were reversed and a customized ANN with ten hidden layers was applied to recognize different patterns. Finally, linear regression was also performed to analyse the relationship between both datasets.

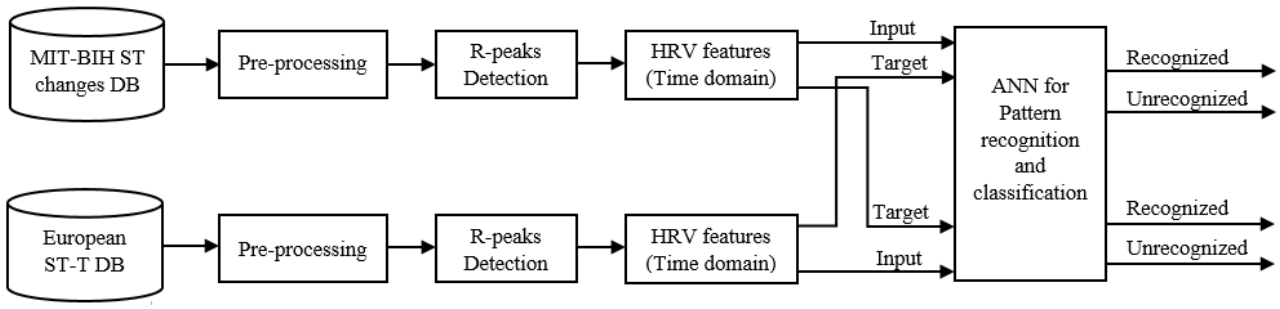

Figure-1. Operational Investigation of the proposed methodology

R-peaks Detection: R-peaks were detected using the software RRAPET (McConnell *et al*., 2020) that was implemented in python and freely available. It took ECG signal (*.dat) as input along with an annotations file (*.atr) and detected R-peaks based on Hilbert transform and variable thresholding. HRV parameters can be calculated by taking just the ECG signal as input whereas to detect R-peaks, an annotation file corresponding to each input ECG signal was required. So, we have used both data sets having annotation files. It took both files (data file and annotation file) as input and gave edited annotations, detected R-peaks, and HRV metrics calculation based on detected R-peaks as output as shown in Figure 2. For R-peaks detection, input was ECG data and pre-processing was performed to remove power line interferences and baseline wanders. The baseline wanders usually range from 0.5Hz to 0.75Hz which occur due to the movement of the body or due to stress. As records from MIT-BIH ST changes database were recorded during an exercise test and exhibited ST-elevation, these morphological changes didn't originate from the cardiac system and required removal to diagnose cardiac diseases easily. Therefore, these low-frequency ST-segments were suppressed by removing baseline wanders. A linear time-invariant high-pass filter with a cut-off frequency of 0.5 Hz was used to remove baseline wander. To overcome the effects of power line interference, a band-pass filter was used. After pre-processing, the ECG signal was analysed in the frequency domain to rectify the phase and to enhance the R-peaks using Hilbert transform. Subsequently, the thresholding was used to detect R-peaks.

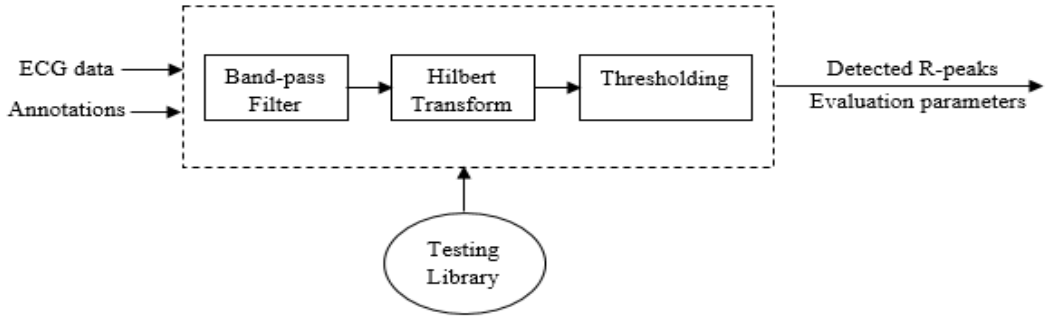

Figure-2. R-peaks detection process of the proposed methodology

The "Testing Library" was used to analyse the performance of the R-peaks detection algorithm. Peaks were detected using merely detected R-peaks from the input signal and R-peaks annotations without any manual editing during pre-processing. Therefore, a beat-to-beat comparison was performed to compare the detected R-peaks with annotations of R-peaks provided with the data file. The comparison classified the R-peaks into three categories: True Positives (TP), False Positives (FP), and False Negatives (FN). If a detected R-peak occurred within the precision window (default value of 0.15s is used) (McConnell *et al*., 2020) of the annotated R-peak, it was categorized as TP. If an R-peak was detected at a location where no R-wave existed, it was classified as FP whereas an R-peak was classified as FN, if an R-peak existed whereas the algorithm didn't detect that R-peak.

HRV Analysis: After R-peaks detection, the next step was feature engineering to extract time-domain measures of HRV analysis. HRV features were extracted based on detected R-peaks. Five state-of-the-art time-domain features for short-term HRV analysis were extracted according to the standards (Camm *et al*., 1996): standard deviation of NN intervals (SDNN), the standard deviation of average NN intervals (SDANN), mean of successive RR intervals (mean RR), root mean square of successive difference (RMSSD) and proportion of the number of RR pairs of successive difference more than 50 ms divided

by the total number of RR intervals (pNN50 %).

Artificial Neural Network: An artificial neural network (ANN) is a structure composed of several interconnected processing units, called neurons similar to the human brain. These large number of interlinked neurons work together to solve a specific problem. There are three types of layers: an input layer, a hidden layer, and an output layer. The input layer is the number of inputs to the neural network whereas hidden layers process the inputs and give an output. Each hidden layer can have a different activation function that decides whether a neuron should activate or not and activated neurons process the input and convert it into output. For the proposed ANN, ten hidden layers were used for better performance after performing grid search. To train the model, the Levenberg-Marquardt algorithm was used for optimal results whereas data was divided randomly. Moreover, cross-entropy was used to measure the pattern recognition performance of the model.

EXPERIMENTAL SETUP, RESULTS AND DISCUSSION: R-peaks detection was the basic step of the proposed methodology. Therefore, R-peaks were detected for twenty records from MIT-BIH ST-changes dataset and twenty records from European ST-T Database using Hilbert transform, and efficiency parameters were calculated. The sampling rate of signals from MIT-BIH ST-changes dataset was 360 Hz whereas, for European ST-T Database, the sampling rate was 250 Hz. As a sampling rate of 250 Hz is adequate to extract HRV measures, therefore, signals from the European dataset were resampled at 250 Hz before R-peaks detection. Patients' details including gender, age, symptoms, and recording lead are available for European ST-T Database whereas for MIT-BIH ST-changes dataset, only lead information is available and patients' details are missing. Therefore, this information is not considered and targeted only R-peaks and evaluation matrices as we have to analyse HRV measures based on these detected R-peaks. Table 1 shows the subjects and evaluation parameters for both databases. The same precision window of 0.15 sec was used for both datasets to detect actual R-peaks from all records.

To evaluate the performance of the R-peaks detection algorithm, four metrics, sensitivity (Sn), positive predictability (PP), accuracy (Ac), and detection error rate (ERd) were assessed by using TP, FP, and FN detections. The evaluation metrics were calculated using the following formulas:

$$Sn = \frac{TP}{TP + FN} \times 100\% \quad (5)$$

$$PP = \frac{TP}{TP + FP} \times 100\% \quad (6)$$

$$Ac = \frac{TP}{TP + FP + FN} \times 100\% \quad (7)$$

$$ERd = \frac{FP + FN}{TP + FN} \times 100\% \quad (8)$$

Table 1. Efficiency parameters computed for R-peaks detection from both datasets.

MIT-BIH ST changes dataset					European ST-T changes dataset				
Subject	Sn	PP	Ac	ERd	Subject	Sn	PP	Ac	ERd
300	100.00	99.96	99.96	0.04	e0103	99.79	99.95	99.74	0.26
301	99.88	99.72	99.60	0.40	e0104	99.91	99.71	99.62	0.38
302	99.67	99.53	99.20	0.81	e0105	99.86	99.70	99.56	0.44
303	99.97	99.50	99.47	0.53	e0108	99.98	91.33	91.32	9.51
304	100.00	99.84	99.84	0.16	e0110	99.37	99.84	99.57	0.43
306	100.00	99.98	99.98	0.02	e0113	99.62	99.59	99.21	0.80
307	99.80	99.27	99.08	0.93	e0114	99.87	99.53	99.41	0.60
308	99.30	98.36	97.69	2.37	e0115	99.98	99.99	99.97	0.03
309	100.00	99.98	99.98	0.02	e0121	99.92	99.98	99.91	0.09
310	100.00	100.00	100.00	0.00	e0122	99.97	99.99	99.96	0.04
311	99.97	99.80	99.77	0.23	e0123	99.99	99.99	99.98	0.02
312	99.15	97.81	96.99	3.10	e0124	99.97	100.00	99.97	0.03
313	99.85	99.74	99.59	0.41	e0125	100.00	99.98	99.98	0.02
314	99.86	99.02	98.88	1.13	e0126	100.00	99.99	99.99	0.01
315	98.90	98.96	97.99	2.16	e0127	100.00	100.00	100.00	0.00
316	99.97	99.94	99.91	0.09	e0133	99.71	99.41	99.12	0.89
317	99.93	99.78	99.71	0.29	e0136	100.00	100.00	100.00	0.00
318	99.24	99.07	99.32	1.71	e0139	99.79	99.95	99.75	0.25
320	99.94	99.84	99.78	0.22	e0147	99.97	99.97	99.94	0.06
321	99.95	99.67	99.62	0.38	e0148	99.34	99.25	98.60	1.42
Average	99.77	99.49	99.32	0.75	Average	99.85	99.41	99.28	0.76

We have detected R-peaks with averaged 99.77% Sn, 99.49% PP and 99.32% Ac for MIT-BIH ST changes data set whereas for European ST-T changes data set, 99.85% Sn, 99.41% PP, and 99.28% Ac was achieved as shown in Table 1.

The further part of the study involved HRV analysis based on these detected R-peaks. For HRV analysis, five time-domain features were extracted for selected twenty records from each dataset. HRV analysis features for both datasets, MIT-BIH ST changes and European ST-T changes, are shown in Table 2.

Table 2. HRV analysis parameters computed for both datasets based on detected R-peaks.

MIT-BIH ST changes dataset						European ST-T changes dataset					
Patient	SDNN	SDANN	mean RR	RMSSD	pNN50%	Patient	SDNN	SDANN	mean RR	RMSSD	pNN50%
300	59.29	32.65	839.24	26.45	0.31	e0103	80.76	67.12	988.39	112.07	16.60
301	280.20	92.75	1120.17	75.09	11.12	e0104	145.86	70.75	933.68	64.29	14.63
302	212.62	73.68	964.99	58.13	5.86	e0105	79.15	55.65	1084.41	44.48	6.02
303	95.23	66.21	969.27	85.93	6.23	e0108	246.76	161.37	996.93	216.98	35.05
304	221.57	74.05	1409.73	52.92	5.01	e0110	136.65	100.44	1008.09	112.15	20.48
306	299.05	65.89	889.56	28.96	8.58	e0113	118.58	69.41	804.57	54.48	9.55
307	277.41	146.03	1282.06	99.68	28.77	e0114	169.50	112.86	1294.66	126.51	33.64
308	285.47	147.79	1092.62	184.03	42.09	e0115	84.56	41.85	636.37	15.26	0.89
309	185.34	49.77	695.34	26.81	4.68	e0121	117.97	55.40	678.08	84.98	1.68
310	129.15	51.33	682.18	12.09	0.79	e0122	30.96	24.59	634.02	29.29	0.38
311	203.94	66.84	874.09	36.59	2.39	e0123	126.26	67.94	751.18	121.57	12.36
312	230.68	104.58	1015.92	118.59	9.02	e0124	167.48	130.38	719.55	175.37	22.57
313	221.65	89.66	741.41	50.74	4.47	e0125	96.07	74.72	782.22	88.81	15.70
314	224.42	93.93	1053.89	80.21	6.97	e0126	79.18	51.25	863.39	74.16	12.15
315	150.20	67.42	692.80	54.44	4.58	e0127	106.46	79.62	767.92	117.38	13.64
316	154.76	48.35	662.18	16.81	1.19	e0133	157.78	114.48	1096.91	155.54	29.98
317	230.60	69.72	860.17	47.51	2.70	e0136	177.48	154.62	1016.97	127.08	31.64
318	120.68	53.26	662.57	57.25	4.35	e0139	116.36	83.75	676.09	109.75	29.83
320	172.69	65.53	886.43	38.36	6.12	e0147	111.40	83.56	1130.57	110.25	53.36
321	174.38	63.42	932.15	39.36	2.83	e0148	251.16	177.95	1083.51	287.08	33.38

Furthermore, data fusion of these HRV analysis features was performed in two scenarios and ANN was applied to efficiently recognize patterns from the two datasets. In scenario 1, HRV measures extracted from MIT-BIH ST changes dataset were selected as input whereas HRV measures extracted from European ST-T changes were selected as the target. Thus, in the first scenario, ST changes are matched with non-specific ST-T changes to recognize patterns from both datasets. In this scenario, patterns from both datasets were recognized accurately >99%. Figure(s) 3a-d presents different efficiency gauges of scenario 1 and highlights the similarity between ST changes and ST-T changes including T-Wave alterations. Figure 3a

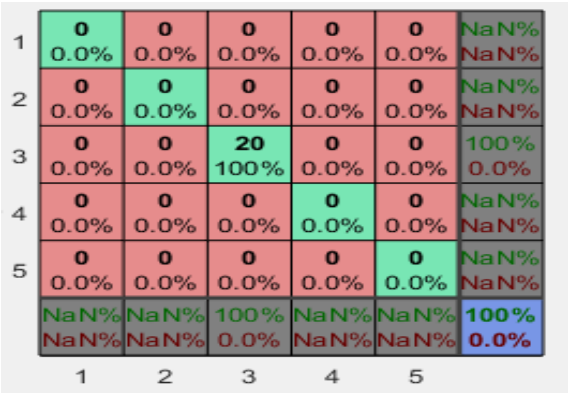

(a) Confusion matrix

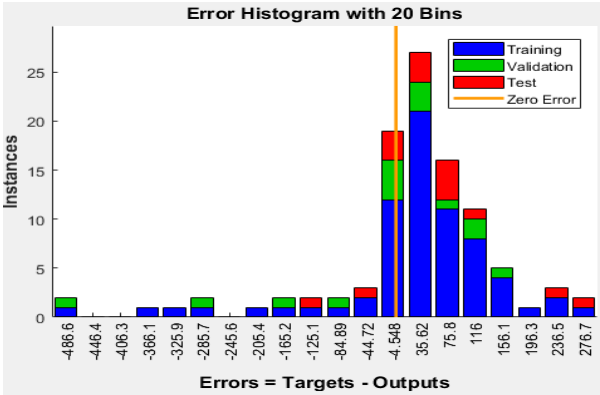

(b) Error Histogram

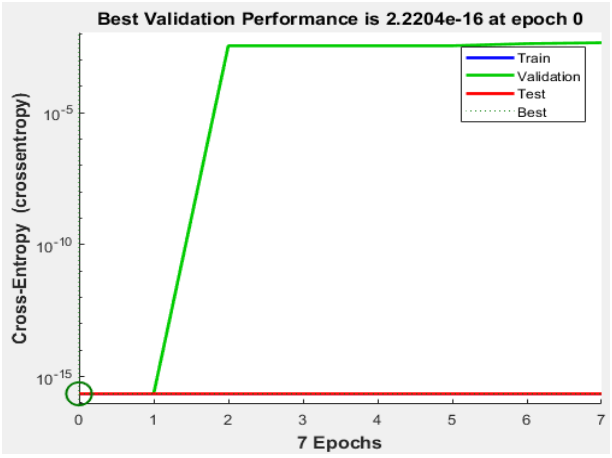

(c) Validation Performance

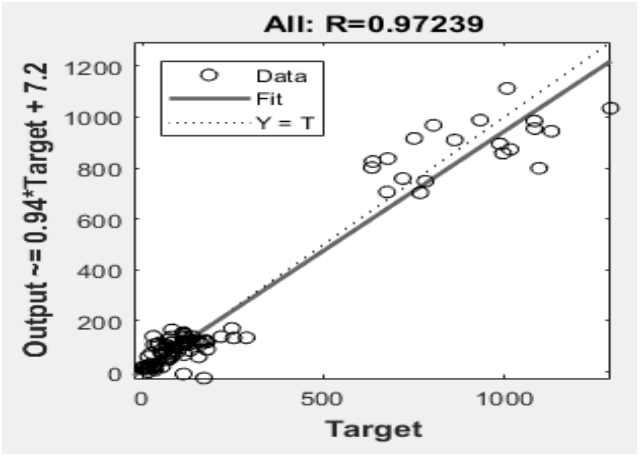

(d) Regression Model

Fig. 3. Findings of scenario 1: (a) confusion matrix highlighting >99% accuracy, (b) error histogram, (c) validation performance of patterns matching ST changes and ST-T changes having ST elevation, depression and T-wave alterations, (d) regression model showing similarity between patterns of both datasets

(a) Confusion matrix

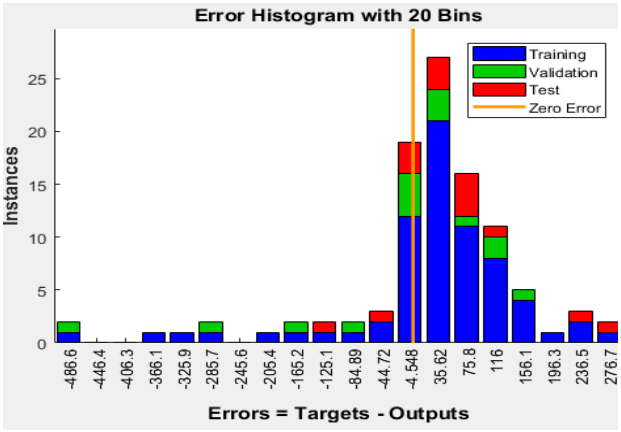

(b) Error Histogram

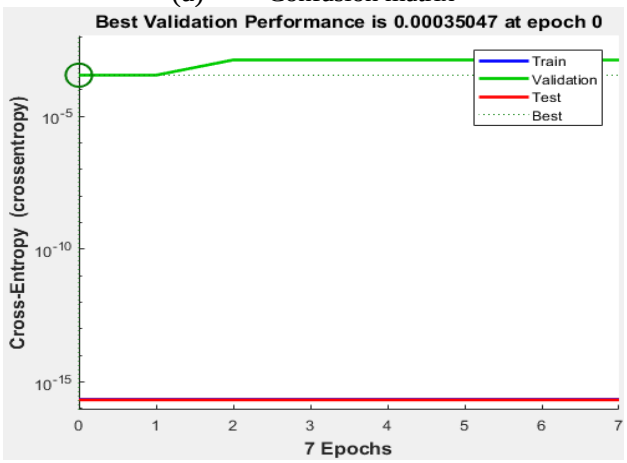

(c) Validation Performance

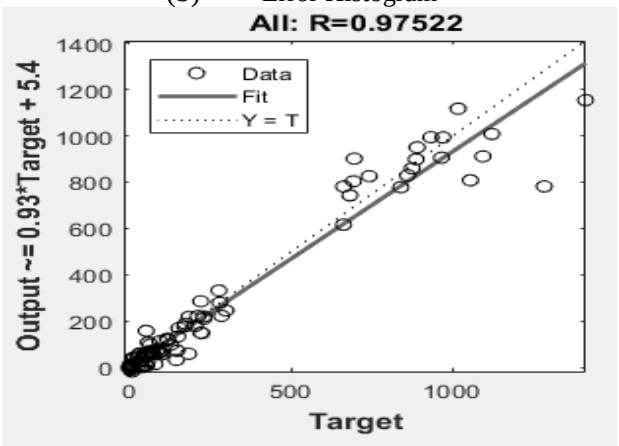

(d) Regression Model

Fig. 4. Findings of scenario 2: (a) confusion matrix highlighting 99% accuracy, (b) error histogram, (c) validation performance of patterns matching ST-T changes including ST elevation, depression and T-wave alterations with MIT-BIH ST changes and, (d) regression model showing similarity of 97% between patterns of both datasets

Shows a confusion matrix with >99% matching of patterns after the fusion of HRV features. Figure 3b presents an error histogram with 20 bins whereas Figure 3c shows the performance evaluation in terms of the best validation point at the level of epoch 0. Linear regression is also performed to analyse the relationship between both datasets that is shown in Figure 3d with an R-value of 0.972.

In scenario 2, HRV features from European ST-T changes dataset were selected as input whereas features from MIT-BIH ST changes dataset were selected as the target. Thus, in the second scenario, ST changes and T-wave alterations from European ST-T changes dataset were matched with ST changes of MIT-BIH dataset to recognize patterns from both datasets. We obtained >99% accuracy in recognizing patterns from both datasets using ANN in this scenario, too. Figure(s) 4a-d presents different efficiency gauges of scenario 2 and highlights the similarity between ST-T changes and ST changes. Figure 4a shows a confusion matrix with >99% matching of patterns after the fusion of HRV features. Figure 4b presents an error histogram with 20 bins whereas Figure 4c shows the performance evaluation in terms of best validation point at epoch 0. Figure 4d shows linear regression results with R-value of 0.975.

Finally, Table 3. summarizes the study presenting different factors used for pattern recognition in both scenarios. i.e. training algorithm, evaluation parameters, ANN layers used, and the fitting model used for evaluating the relationship between both datasets.

Table 3. Summary of both scenarios in terms of input, training and output factors.

Factors	Scenario 1	Scenario 2
Data division	Random	Random
Training Algorithm	Levenberg-Marquardt	Levenberg-Marquardt
Performance measuring parameter	Cross entropy	Cross entropy
ANN layers (input/hidden/output)	5/10/5	5/10/5
Epochs	7	7
Accuracy (confusion matrix)	>99%	>99%
Error histogram (bins)	20	20
Best validation performance (epoch)	2.2204E-16 (0)	0.00035047 (0)
Similarity index (Regression Model)	0.97239	0.97522

DISCUSSION

Different studies have used different techniques to improve the accuracy of R-peaks detection, as R-peaks detection from the ECGs is the very first part of HRV analysis. The more reliable detection of R-peaks results in better HRV analysis leading to better analysis and detection of any cardiac disease. According to (Sanjee, 2010) the QRS complex and especially R-peaks detection rather than other morphological markers is the most significant driving factor to diagnosis a cardiac disease. The number of R-peaks in a specific time interval computes to HR and variations in successive RR interval indicates HRV that is clinically a significant factor. Numerous studies have performed HRV analysis based on R-peaks detection to detect different CVDs. (Acharya *et al*., 2008) reviewed studies performing HRV analysis to analyse and classify different cardiac diseases. They also performed HRV analysis to predict the risk of CVDs where the initial step for their study as well as studies included in the review, was R-peaks detection. (Sunkaria *et al*., 2010) concluded that reliable detection of R-peaks and RR interval computation has been proved effective in the reliable evaluation of HRV parameters. They used symmetric wavelets to detect R-peaks from standard datasets as well as self-recorded ECGs of healthy subjects and depressed patients and performed HRV analysis. According to (Nouira *et al*., 2013) ECG is a significantly used tool to diagnose arrhythmia that depends upon reliable R-peaks detection and analysis of RR interval to find out the irregularity. Discrete Wavelet Transform (DWT) was applied to detect R-peaks and subsequently, three methods; the standard deviation of HR, Fast Fourier Transform (FFT), and the Wavelet Transform were applied on detected RR intervals to perform HRV analysis.

MI occurs due to blockage in blood vessels supplying blood to heart muscles. This blockage causes irregularity in heartbeats resulting in unusual abnormalities in the ECG of a patient. These abnormalities may result in bradycardia or tachycardia that can be identified by analysing morphological changes in the P wave, QRS complex, T, and U wave. The most important feature to detect MI is QRS complex detection and RR intervals to analyse the type of irregularity, which depends upon the R-peaks detection. The detected R-peaks are further used to analyse changes in ST-segment and T wave. Reliable and accurate detection of R-peaks leads to the diagnosis of MI correctly (Kora and Kalva, 2015). (Acharya *et al*., 2017a) applied the Pan-Tompkins algorithm to detect R-

peaks and applied Discrete Wavelet Transform (DWT), Empirical Mode Decomposition (EMD), and Discrete Cosine Transform (DCT) to classify normal, coronary artery disease, and MI. They achieved an accuracy of 98.5% due to the accurate detection of R-peaks. In another study, they classified normal and MI beats by applying CNN without performing R-peaks detection but could achieve accuracy up to 93.5% (Acharya *et al*., 2017b). This significant difference in accuracy for both studies highlights the importance of R-peaks detection in the diagnosis of any cardiac disease. (Al-Kindi and Tafreshi, 2011) proposed an algorithm to detect MI in real-time by analysis of ST-segment, continuously. The algorithm was dependent upon R-peaks detection as features of interest i.e. QRS complex and j point was extracted to measure ST elevation and depression. According to clinical guidelines of MI prognosis, both are important indicators of MI presence. The algorithm detected MI with 85% sensitivity. (Liu *et al*., 2015) presented an ECG curve fitting and detected MI accurately up to 94.4%. Though the signals had weak or undetectable ST segments, the ST segments were measured using detected R-peaks as a reference point. ECG signals were split into cycles of PQRST waves and R-peaks were selected as ECG cycle boundaries and to measure ST segments. According to the referred studies, reliable and accurate detection of R-peaks is the main task in HRV analysis to analyse cardiovascular diseases including MI.

Finally, Table. 4 summarises a few recent studies performing HRV analysis to detect different cardiovascular diseases. (Hirsch *et al*., 2020) detected R-peaks from ECG signals and extracted features based on detected RRI series. The extracted features were fed into three classifiers where random forest outperformed the other two classifiers and detected AF with accuracy of 97.4%. (Rohila and Sharma, 2020) computed RR intervals from 5 min ECGs by detecting R-peaks. Based on these detected intervals, HRV analysis features including time-frequency domain features and some non-linear features were computed to detect SCD. SVM and DT were applied and DT classified SCD accurately up to 91.67% from CAD and CHF patients.(Taye *et al*., 2020) detected QRS complex to find R-peaks and extracted HRV analysis features using the detected R-peaks. 11 linear and non-linear features were extracted from 5 min ECG and fed into three machine learning (ML) classifiers and CNN to predict VTA. CNN predicted VTA with highest accuracy of 84.6% as compared to other ML classifiers. (Shi *et al*., 2019) extracted some statistical features as well as HRV features followed by QRS complex detection. They also suggested a novel entropy, Renyi Distribution Entropy (RdisEn) to perform short-term HRV analysis and detected CAD. KNN and SVM were applied on selected features, and KNN detected CAD from healthy subjects with accuracy of 97.5%, using only 5 features. (Isler *et al*., 2019) extracted linear and non-linear HRV features following R-peaks detection and classified CHF patients from healthy controls by applying a 3-stage classifier. Five classifiers were employed.

Table 4. Summary of studies performing HRV analysis to classify different CVDs.

Author(s)	Disease	Features	Method	Accuracy
(Hirsch *et al*., 2020)	AF	RRI time series	RF	97.4%
(Rohila and Sharma, 2020)	SCD	Entropy, Poincare plot, S-transform	SVM and DT	91.67%
(Taye *et al*., 2020)	VTA	Linear and Nonlinear HRV analysis features	CNN	84.6%
(Heng *et al*., 2020)	VF	Time domain and nonlinear HRV analysis features	SVM	94.7%
(Shi *et al*., 2019)	CAD	RdisEn and WPD (statistical features)	KNN and SVM	97.5%
(Isler *et al*., 2019)	CHF	Linear and Nonlinear HRV analysis features	3 stage Classifier	98.8%
Proposed Model	MI	Time domain HRV analysis features	Customized ANN	>99%

AF: Atrial fibrillation, CAD: Coronary Artery Disease, CHF: Congestive Heart Failure, VTA: Ventricular Tachyarrhythmia, VF: Ventricular Fibrillation, MI: Myocardial Infarction, RdisEn: Renyi distribution entropy, WPD: Wavelet Packet Decomposition, RF: Random Forest, SVM: Support Vector Machine, DT: Decision Tree, CNN: Convolutional Neural Network, KNN: K-Nearest Neighbour, ANN: Artificial Neural Network on different combinations of these features and among which multilayer perceptron (MLP) classified CHF patients with an accuracy of 98.8%. All of these studied extracted HRV analysis features based on reliable R-peaks detection and achieved satisfactory results for detection and classification CVDs. Similarly, to highlight importance of reliable R-peaks detection we have detected MI by recognizing different patterns from ECG signal having non-specific abnormalities like ST-T changes. MI patterns were recognized with accuracy of greater than 99% as R-peaks were detected with 99% accuracy that specifies accurate detection of R-peaks as the base for excellent HRV and CVDs analysis.

Conclusion and Future Work: The proposed research

work measured the interdependence of HRV analysis and R-peaks. For assessment, ECG signals having non-specific abnormalities like ST changes and T-wave alternans were used from two publicly available datasets and HRV analysis was performed to recognize patterns of cardiac disease, MI. The initial point was the reliable detection of R-peaks with higher accuracy and sensitivity. R-peaks are detected with >99% accuracy, sensitivity, and positive predictability for both datasets. Subsequently, short-term HRV analysis parameters from the time domain are computed for both datasets based on the detected R-peaks. Afterward, to assess the importance of reliable detection of R-peaks for HRV analysis, data fusion of these HRV parameters computed from both datasets was performed in two scenarios. A finely tuned ANN with ten hidden layers was applied for pattern recognition and an accuracy greater than 99% was achieved in both scenarios. Furthermore, linear regression was also performed on computed HRV measures in both scenarios that observed similarity of 97% between both datasets. In the end, the importance of R-peaks detection for HRV analysis to analyse different cardiovascular diseases was elaborated from the literature.

The limitations of this study was that we have used just time-domain measures for HRV analysis as we intended to focus mainly on the importance of R-peaks detection in HRV analysis. In the future, we call for research to perform HRV analysis of ECG signals to detect and classify MI. Further, frequency domain and non-linear parameters in conjunction with time-domain parameters may also be used for the detection and recognition of the aforementioned cardiac disease. Furthermore, just forty records are included in the study, therefore, the methodology may be applied to a large dataset to verify the results.

Ethical Clinical Statement: The approach adopted in this study to diagnose the cardiac disease has purely followed the ethical standards under the 1964 Helsinki declaration.

REFERENCES

Acharya, U. R., Fujita, H., Adam, M., Lih, O. S., Sudarshan, V. K., Hong, T. J., Koh, J. E., Hagiwara, Y., Chua, C. K. and Poo, C. K. (2017a). Automated characterization and classification of coronary artery disease and myocardial infarction by decomposition of ECG signals: A comparative study. Information Sciences. 377: 17-29.

Acharya, U. R., Fujita, H., Oh, S. L., Hagiwara, Y., Tan, J. H. and Adam, M. (2017b). Application of deep convolutional neural network for automated detection of myocardial infarction using ECG signals. Information Sciences. 415: 190-198.

Acharya, U. R., Joseph, K. P., Kannathal, N., Lim, C. M. and Suri, J. S. (2006). Heart rate variability: a review. Medical and biological engineering and computing. 44(12): 1031-1051.

Acharya, U. R., Sankaranarayanan, M., Nayak, J., Xiang, C. and Tamura, T. (2008). Automatic identification of cardiac health using modeling techniques: A comparative study. Information Sciences. 178(23): 4571-4582.

Ahmed, D. M. (2015). What's a NSTEMI? Non ST Segment Myocardial Infarction [Online]. MYHEART.NET. Available: https://myheart.net/articles/nstemi/ [Accessed 12 February 2021].

Al-Kindi, S. G. and Tafreshi, R. (2011). Real-time detection of myocardial infarction by evaluation of ST-segment in digital ECG. Journal of Medical Imaging and Health Informatics. 1(3): 225-230.

Al-Zaiti, S., Callaway, C., Lux, R., Nemec, J., Sejdic, E., Soman, P. and Walden, K. (2017). Spatial indices of repolarization correlate with non-ST elevation myocardial ischemia in patients with chest pain. Journal of Electrocardiology. 50(6): 864.

Albrecht, P. 1983. ST segment characterization for long term automated ECG analysis. Massachusetts Institute of Technology, Department of Electrical Engineering ….

Anderson, J. L. and Morrow, D. A. (2017). Acute myocardial infarction. New England Journal of Medicine. 376(21): 2053-2064.

Aro, A. L., Anttonen, O., Tikkanen, J. T., Junttila, M. J., Kerola, T., Rissanen, H. A., Reunanen, A. and Huikuri, H. V. (2012). Prevalence and prognostic significance of T-wave inversions in right precordial leads of a 12-lead electrocardiogram in the middle-aged subjects. Circulation. 125(21): 2572-2577.

Baloglu, U. B., Talo, M., Yildirim, O., San Tan, R. and Acharya, U. R. (2019). Classification of myocardial infarction with multi-lead ECG signals and deep CNN. Pattern Recognition Letters. 122: 23-30.

Basit, H., Malik, A. and Huecker, M. (2019). Non ST Segment Elevation (NSTEMI) Myocardial Infarction [Updated 2019 May 4]. StatPearls [Internet]. Treasure Island (FL): StatPearls Publishing.

Benjamin, E. J., Muntner, P., Alonso, A., Bittencourt, M. S., Callaway, C. W., Carson, A. P., Chamberlain, A. M., Chang, A. R., Cheng, S. and Das, S. R. (2019). Heart disease and stroke Statistics-2019 update a report from the American Heart Association. Circulation.

Butun, E., Yildirim, O., Talo, M., Tan, R.-S. and Acharya, U. R. (2020). 1D-CADCapsNet: One dimensional deep capsule networks for coronary artery disease detection using ECG signals. Physica Medica. 70: 39-48.

Camm, A. J., Malik, M., Bigger, J. T., Breithardt, G., Cerutti, S., Cohen, R. J., Coumel, P., Fallen, E. L., Kennedy, H. L. and Kleiger, R. (1996). Heart rate variability: standards of measurement, physiological interpretation and clinical use. Task Force of the European Society of Cardiology and the North American Society of Pacing and Electrophysiology.

Chanwimalueang, T., von Rosenberg, W. and Mandic, D. P. Enabling R-peak detection in wearable ECG: Combining matched filtering and Hilbert transform. 2015 IEEE International Conference on Digital Signal Processing (DSP), 2015. IEEE, 134-138.

Chen, X., Yang, R., Ge, L., Zhang, L. and Lv, R. (2017). Heart rate variability analysis during hypnosis using wavelet transformation. Biomedical Signal Processing and Control. 31: 1-5.

Clinic, C. Coronary Artery Disease [Online]. Cleveland Clinic. Available: https://my.clevelandclinic.org/health/diseases/16898-coronary-artery-disease [Accessed 12 February 2021].

D'Aloia, M., Longo, A. and Rizzi, M. (2019). Noisy ECG signal analysis for automatic peak detection. Information. 10(2): 35.

Hamilton, P. S. and Tompkins, W. J. (1986). Quantitative investigation of QRS detection rules using the MIT/BIH arrhythmia database. IEEE transactions on biomedical engineering. (12): 1157-1165.

He, R., Wang, K., Li, Q., Yuan, Y., Zhao, N., Liu, Y. and Zhang, H. (2017). A novel method for the detection of R-peaks in ECG based on K-Nearest Neighbors and Particle Swarm Optimization. EURASIP Journal on Advances in Signal Processing. 2017(1): 82.

Heng, W. W., Ming, E. S. L., Jamaluddin, A. N. B., Harun, F. K. C., Abdul-Kadir, N. A. and Yeong, C. F. Prediction of Ventricular Fibrillation Using Support Vector Machine. IOP Conference Series: Materials Science and Engineering, 2020. IOP Publishing, 012008.

Hirsch, G., Jensen, S. H., Poulsen, E. S. and Puthusserypady, S. (2020). Atrial Fibrillation Detection Using Heart Rate Variability and Atrial Activity: A Hybrid Approach. Expert Systems with Applications. 114452.

Iqbal, U., Wah, T. Y., ur Rehman, M. H., Mujtaba, G., Imran, M. and Shoaib, M. (2018). Deep deterministic learning for pattern recognition of different cardiac diseases through the internet of medical things. Journal of medical systems. 42(12): 252.

Isler, Y., Narin, A., Ozer, M. and Perc, M. (2019). Multi-stage classification of congestive heart failure based on short-term heart rate variability. Chaos, Solitons & Fractals. 118: 145-151.

John, A. A., Subramanian, A. P., Jaganathan, S. K. and Sethuraman, B. (2015). Evaluation of cardiac signals using discrete wavelet transform with MATLAB graphical user interface. Indian heart journal. 67(6): 549-551.

Jovic, A., Brkic, K. and Krstacic, G. (2019). Detection of congestive heart failure from short-term heart rate variability segments using hybrid feature selection approach. Biomedical Signal Processing and Control. 53: 101583.

Kaur, H. and Rajni, R. (2017). Electrocardiogram signal analysis for R-peak detection and denoising with hybrid linearization and principal component analysis. Turkish Journal of Electrical Engineering & Computer Sciences. 25(3): 2163-2175.

Kora, P. and Kalva, S. R. (2015). Improved Bat algorithm for the detection of myocardial infarction. SpringerPlus. 4(1): 666.

Lee, M., Park, D., Dong, S.-Y. and Youn, I. (2018). A novel R peak detection method for mobile environments. IEEE Access. 6: 51227-51237.

Liu, B., Liu, J., Wang, G., Huang, K., Li, F., Zheng, Y., Luo, Y. and Zhou, F. (2015). A novel electrocardiogram parameterization algorithm and its application in myocardial infarction detection. Computers in biology and medicine. 61: 178-184.

Lodhi, A. M., Qureshi, A. N., Sharif, U. and Ashiq, Z. A novel approach using voting from ecg leads to detect myocardial infarction. Proceedings of SAI Intelligent Systems Conference, 2018. Springer, 337-352.

McConnell, M., Schwerin, B., So, S. and Richards, B. (2020). RR-APET-Heart rate variability analysis software. Computer methods and programs in biomedicine. 185: 105127.

Nouira, I., Abdallah, A. B., Bedoui, M. H. and Dogui, M. (2013). A Robust R Peak Detection Algorithm Using Wavelet Transform for Heart Rate Variability Studies. International Journal on Electrical Engineering & Informatics. 5(3).

Organization, W. H. (2017). Cardiovascular diseases (CVDs) : Key Facts [Online]. World Health Organization. Available: https://www.who.int/news-room/fact-sheets/detail/cardiovascular-diseases-(cvds) [Accessed 23 January 2021].

Pan, J. and Tompkins, W. J. (1985). A real-time QRS detection algorithm. IEEE transactions on

biomedical engineering. (3): 230-236.

Pang, D. and Igasaki, T. (2018). A Combined Syntactical and Statistical Approach for R Peak Detection in Real-Time Long-Term Heart Rate Variability Analysis. Algorithms. 11(6): 83.

PhysioNet. PhysioNet: The Research Resource for Complex Physiologic Signals [Online]. PhysioNet. Available: https://physionet.org/.

Prasad, S. T. and Varadarajan, S. (2013). Heart rate detection using Hilbert transform. International Journal of Research in Engineering and Technology. 2(8): 12-18.

Prutkin, J. M. (May 2020). NONSPECIFIC ST-T WAVE CHANGES [Online]. UpToDate. Available: https://www.uptodate.com/contents/ecg-tutorial-st-and-t-wave-changes#H1 [Accessed 02 February 2021].

Qin, Q., Li, J., Yue, Y. and Liu, C. (2017). An adaptive and time-efficient ECG R-peak detection algorithm. Journal of Healthcare Engineering. 2017.

Rakshit, M., Panigrahy, D. and Sahu, P. (2016). An improved method for R-peak detection by using Shannon energy envelope. Sādhanā. 41(5): 469-477.

Rivero, D., Alhamaydeh, M., Faramand, Z., Alrawashdeh, M., Martin-Gill, C., Callaway, C., Drew, B. and Al-Zaiti, S. (2019). Nonspecific electrocardiographic abnormalities are associated with increased length of stay and adverse cardiac outcomes in prehospital chest pain. Heart & Lung. 48(2): 121-125.

Rohila, A. and Sharma, A. (2020). Detection of sudden cardiac death by a comparative study of heart rate variability in normal and abnormal heart conditions. Biocybernetics and Biomedical Engineering. 40(3): 1140-1154.

Sabherwal, P., Agrawal, M. and Singh, L. (2017). Automatic detection of the R peaks in single-lead ECG signal. Circuits, Systems, and Signal Processing. 36(11): 4637-4652.

Sanjee, S. R. ECG Feature Detection Using SAS®. Proceedings of the 2010 Conference of the Pharmaceutical Industry SAS Users Group, Cary, NC: SAS Institute, Inc, 2010.

Sharma, L. D. and Sunkaria, R. K. (2016). A robust QRS detection using novel pre-processing techniques and kurtosis based enhanced efficiency. Measurement. 87: 194-204.

Shi, M., Zhan, C., He, H., Jin, Y., Wu, R., Sun, Y. and Shen, B. (2019). Renyi distribution entropy analysis of short-term heart rate variability signals and its application in coronary artery disease detection. Frontiers in physiology. 10: 809.

Sunkaria, R. K., Saxena, S. C., Kumar, V. and Singhal, A. M. (2010). Wavelet based R-peak detection for heart rate variability studies. Journal of medical engineering & technology. 34(2): 108-115.

Taddei, A., Distante, G., Emdin, M., Pisani, P., Moody, G., Zeelenberg, C. and Marchesi, C. (1992). The European ST-T database: standard for evaluating systems for the analysis of ST-T changes in ambulatory electrocardiography. European heart journal. 13(9): 1164-1172.

Taye, G. T., Hwang, H.-J. and Lim, K. M. (2020). Application of a convolutional neural network for predicting the occurrence of ventricular tachyarrhythmia using heart rate variability features. Scientific reports. 10(1): 1-7.

Thygesen, K., Alpert, J. S., Jaffe, A. S., Chaitman, B. R., Bax, J. J., Morrow, D. A. and White, H. D. (2018). Fourth universal definition of myocardial infarction (2018). Journal of the American College of Cardiology. 72(18): 2231-2264.

Yakut, Ö. and Bolat, E. D. (2018). An improved QRS complex detection method having low computational load. Biomedical Signal Processing and Control. 42: 230-241.